INSTRUMENTED SOIL REINFORCED RETAINING WALL: ANALYSIS OF MEASUREMENTS AND F.E.M. ANALYSIS

FILIPPO MONTANELLI, ENG.
TENAX SPA, ITALY
NICOLA MORACI, PROF.
UNIVERSITY OF REGGIO CALABRIA
PAOLO CARRUBBA, PROF.
UNIVERSITA' DI PADOVA, ITALY
FAUSTA LUCHETTA, ENG.
UNIVERSITA' DI PADOVA, ITALY

INTRODUCTION

A vertical retaining wall, 4m high and 10m long, was constructed by reinforcing the backfill with geogrids. The reinforcing layers were instrumented with strain gauges, tensile geogrid load transducers and horizontal displacement sensors. In addition, total soil pressure transducers were installed inside the structure to monitor the internal state of stress of the reinforced wall.

The aim of this research is to better understand the behavior of reinforced structures. In particular, the development of slip surfaces and the tensile forces acting in the reinforcements were investigated. By this analysis it was possible to assess current design approaches and related safety factors in terms of either long term tensile failure, pullout, direct sliding or compound failures. Data related to reinforcement tensile strains and loads, applied vertical pressures, rainfall and construction sequences were collected for two different geogrids over a period exceeding 15,000 hours. The experimental data have been compared with output generated by conventional design methodology and output given by F.E.M.

Several design methods, which are based on a limit equilibrium approach, have been proposed to address the uncertainties associated with geosynthetic reinforced structures. (Jewell, et al., 1984; Jewell, 1991; Bonaparte, et al., 1987; Broms, 1988; Collin, 1986; Simac, et al., 1990; Leshchinsky and Perry, 1987; Schmertmann, et al., 1987). These methods consider different hypothesis and failure surfaces. So, the factors of safety against failure vary with the design method used.

This paper discusses an instrumented geosynthetic reinforced wall constructed in Italy near the town of Vicenza (Carrubba et al. (1999)). The structure was monitored from the initial phase of construction, during the service phase and at failure. Serviceability failure was achieved by surcharging the wall with 3.5 m of soil especially in the GG20PP section.

This study provides valuable insight in reinforced wall behavior, including the location of

failure surfaces, tensile stresses and strains distribution, and factors which can affect short and long term factors of safety such as geosynthetic creep and aging, rain effects and consolidation.

This document is a continuation of previously published documents and it contains additional experimental data, better soil parameter definition and testing and results of F.E.M. analysis by mean of Abaqus program (1997).

SOIL AND GEOSYNTHETIC PROPERTIES

The fill soil used for the construction of the wall, is called "Cereda tout venant", and was excavated from a quarry located near the construction site. Ten percent of the soil passes the 0.075 mm sieve. It has a uniformity coefficient (C_u) of 130 and a curvature coefficient (C_c) of 19. The Atterberg limits were evaluated on the fine fraction and are as follows: liquid limit LL = 28, plastic limit PL = 20; and plasticity index PI = 8. According to the unified soil classification system USCS, this soil is a clayey gravel (GC).

Laboratory compaction tests were carried out following the standard and modified AASHTO method. The maximum dry density ($\gamma_{d\ max}$) values were 20.95 and 22.25 kN/m^3 at optimum water content (w_{opt}) of 8.5 % and 5.5 % respectively. In situ determination trials of the soil density have yielded an actual soil density value of 17.7 kN/m^3.

The permeability tests were performed in a triaxial apparatus under constant hydraulic load (corresponding to an hydraulic gradient equal to 1.0) and under confinement pressures of 50 and 100 kPa. The test results of specimens compacted at optimum water content indicate the soil has a permeability coefficient ranging from 2.0 10^{-4} to 2.5 10^{-4} cm/s.

To evaluate the soil's shear strength, different laboratory tests were performed. Triaxial tests (CD) on large diameter specimens (100 mm) were conducted to determine the shear strength at low strain and confining stress levels. The test results indicate a very high shear strength for confining stresses (σ) between 20 kPa and 100 kPa due to the dilatant behavior of the soil subjected to compaction effort. The above tests have yielded a soil friction angle Φ' of 46.5° with a cohesion c' of 5 kPa. The elastic modulus of the reinforced soil has been determined with unload and reload cyclic triaxial test. For design purpose the soil elastic modulus has been determined equal to 50,000 kPa. The at-rest coefficient of thrust k_0 has been determined equal to 0.4 by mean of an edometric test performed in a triaxial cell in which the soil is allowed to consolidate at constant volume.

Direct shear tests were performed on the portion of soil finer then 0.425 mm using the Casagrande shear box and the Bromhead ring shear apparatus to evaluate its large-displacement shear strength. The tests results indicate a residual shear strength angle (coincident with constant volume shear strength angle Φ_{cv}) of approximately 40 degrees.

The wall was built using two different reinforcement geogrids. One section was 5.0m in width

and was reinforced with 3 layers 2.0 m long of a high-density polyethylene (HDPE) uniaxial oriented extruded geogrids. The second section was also 5.0m in width and was reinforced with 3 layers 2.2 m long of a polypropylene (PP) biaxially oriented extruded geogrids. The geogrids' nominal properties are reported in Table 1.

Table 1. Geogrids' nominal properties.

Product Name	Tenax LBO 220 SAMP	Tenax TT 201 SAMP
Product Code	GG20PP	GG45PE
Polymer Type	Polypropylene	High Density Polyethylene
Nominal Tensile Strength, MD	20 kN/m	45 kN/m
Strain at Peak, MD	11%	12%
Tensile Strength at 2% Strain	7 kN/m	13 kN/m
Tensile Strength at 5% Strain	14 kN/m	26 kN/m
Unit Weight	270 g/m^2	450 g/m^2
Mesh Sizes	41 x 31 mm	130 x 15 mm
Junction Strength	18 kN/m	36 kN/m

Pullout tests, in agreement with current ASTM and CEN draft methodology, have been conducted on both geogrids using the actual fill soil. The dimensions of the specimens have been 1 m long by 0.5 m wide. The pullot tests have shown that both the geogrids have a pullout factor f_{po} equal to 1.0.

DESIGN AND CONSTRUCTION

The reinforced wall was designed using a limit equilibrium approach (Leshchinsky 1995) using the RESLOPE design software. An internal soil friction angle (Φ_{cv}) of 40 degrees was used for the reinforced soil design. This value of friction angle, (resulting from the Casagrande direct shear tests conducted on the soil passing 0.425 mm sieve, has been selected since it is the typical value used by geotechnical engineers for design. The two sections of the wall were designed based on to two different failure mechanisms: the tie-back tensile failure for the portion of wall reinforced with GG20PP geogrids and the pullout failure for the other portion reinforced with GG45PE geogrids. All the Safety and Material Factors were deliberately set to 1.00 to design a wall at limit equilibrium stage and consequent failure during surcharge loading.

The long term allowable design tensile strength of the geogrids was assumed to be equal theirs peak tensile strength as determined by the wide width tensile test method (ASTM D4595). Since geogrids with different strengths were used in the design, the vertical spacing and the reinforcement lengths of these two sections were also different. For the section reinforced with GG20PP geogrids, three layers, each 2.20m long, were necessary. The first layer was installed at elevation 0.00m with respect to the base, the second at 0.80m and the third at 2.40m elevation. For the section reinforced with GG45PE geogrids, three layers, each 2.00m long, were necessary.

The first layer was installed at elevation 0.00m with respect to the base, the second at 1.30m and the third at 2.90m elevation.

To ensure the face stability and geometry, the structure was constructed using “left in place” welded wire formworks. They are composed of wire mesh (ϕ = 8 mm, mesh 200 x 200 mm) precut to a height of about 1.5m and bent to the face at an angle of 85 degrees. The fill soil was compacted in layers of 0.3m thick using a vibrating roller (80 kN). The structure, already built with 3.5 m of surcharge, is shown in Figure 1.

Figure 1. Side and front view of the two reinforced wall sections.

The geogrids were instrumented with self-temperature compensated strain gauges having a nominal gauge length of 5mm and a maximum strain of 10% with a measurement accuracy of 0.5%. The strain gauges were glued to the geogrid ribs with cyanoacrylate adhesive using a multi-step method. This procedure allows the measurement of the geogrid strains up to 10%, over a period in excess of two years and during freezing temperatures. Ten strain gauges were installed on each reinforcement layer at a spacing of about 0.20m. The strain gauges were protected with silicon rubber and with a 0.10m-thick sand layer. The effectiveness of this procedure has been demonstrated by the low mortality rate of the sensors (only one out of 63 sensors malfunctioned). The electrical connections were made using a three wires Whetstone quarter bridge. The strain gauges were connected to an automatic data acquisition unit, which is capable of recording up to 100 sensors every 15 minutes. The actual recording frequency was reduced to once per day after the construction was completed.

Additional geogrids specimens, instrumented with strain gauges, were prepared and tested in the laboratory to provide a basis for calibration and correlation between measured strain, true strain and tensile stress. The stress-strain curves and modulus for both geogrids were established with laboratory testing. These relationships are function of time, temperature, stress and strain. The following tests were performed to define the time dependent properties of the geogrids: in

isolation index single rib tensile tests, low strain rate tensile tests, and different load ratio creep tests.

Three tensile load cells, each having a physical profile similar to the shape of the uniaxial geogrid, were installed at each GG45PE reinforcement layer to record the actual confined tensile loads in the material. Three vertical total stress cells, each having a diameter of 300mm, were installed at each GG45PE reinforcement layer to record the actual vertical total stress in soil. These cells were located 1m inside the wall face. Horizontal multiple base displacements sensors were installed on the GG45PE geogrid layers to monitor absolute and differential movements of the reinforced mass and its face.

The wall was constructed in approximately one week and left to rest for about 75 days. Then every about 75 days, it has been loaded with a surcharge of about 1.2 m of fill soil until the overall height of 7.5 m has been reached.

ANALYSIS OF THE RECORDED DATA

The change of total vertical pressures over time at the different reinforcing layers during construction and surcharging is shown in Figure 2 for the section of wall reinforced with GG45PE. These data demonstrate a good response of instrumentation to the vertical pressure changes, even if some discrepancies may be noticed with respect to theoretical values. This behavior may be attributed to the proximity of the cells to face (1.0m), the flexibility effects of the face itself, the position of the cells with respect to the surcharge and finally, to the presence of a rigid base on which the wall was founded.

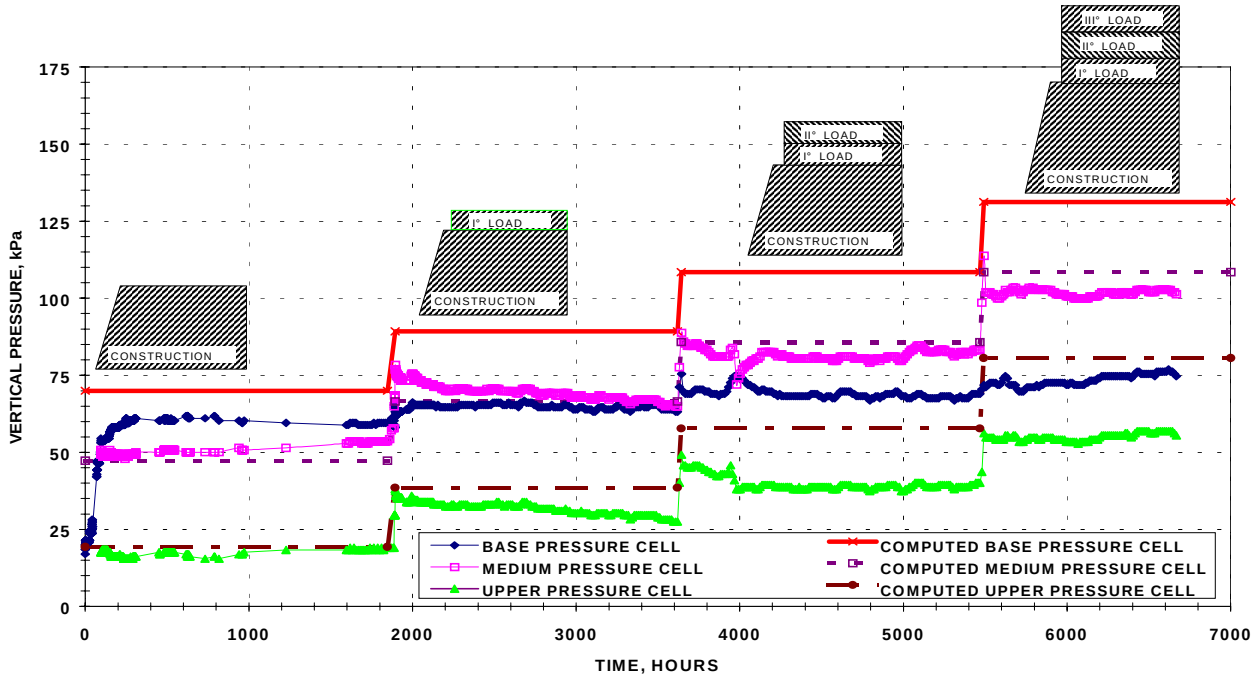

Figure 2. Variation of total vertical pressure during construction and surcharging for the GG45PE geogrid reinforced wall.

The changes of the total vertical pressures over time are compared to the recorded rainfall in Figure 3. The figure shows that the change of the unit weight over time has a little influence on recorded data. A comparison between the applied total vertical pressures and the associated strains in reinforcing layers is shown in Figure 4 for both geogrids. The data in Figures 2 and 3 indicates a good response with respect to time of loading of the two independent monitoring systems. For a given stress level, the dependence of recorded strain on geogrid stiffness is clearly shown in Figure 4.

The effects of the rainfall and consequent pore water pressure increase are clearly visible in figures 3 and 4. At 4,000 hours, the heavy rains have yielded a high increase in horizontal tensile strains (Fig. 4) and consequent reduction in the vertical pressure acting on the pressure cells (fig. 3). This behavior can be explained an increase in horizontal stresses with consequent wall deformation and corresponding rotation of vertical loads in the horizontal direction.

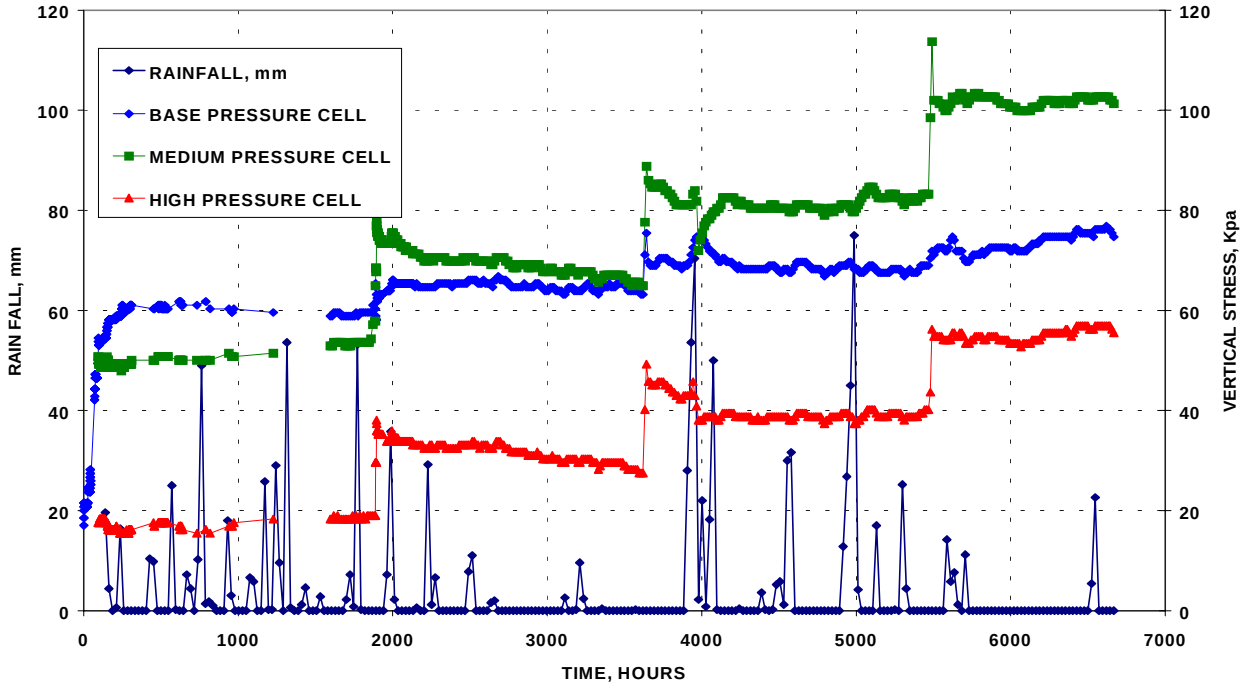

Figure 3. Total vertical pressure and rainfall during construction and surcharging for the GG45PE geogrid reinforced wall.

Figure 5 shows the development of tensile strain over time in the upper layer of both GG45PE and GG20PP. The data indicate a marked dependence of the tensile strain in geogrids on the stress level achieved during surcharging, the geogrid stiffness and its creep properties. Moreover, for a given temperature, creep became more important as the tensile stress in reinforcement increases. Finally, it is possible to observe that the effect of creep is more significant in GG20PP geogrids than in GG45PE geogrids. This is due to the different applied load ratio, polymer, manufacturing process, and the involved failure mechanisms. The development of tensile strains over time for strain gauges located at different locations along the geogrid length is shown Figures 6 and 7 for the GG20PP and the GG45PE geogrids, respectively.

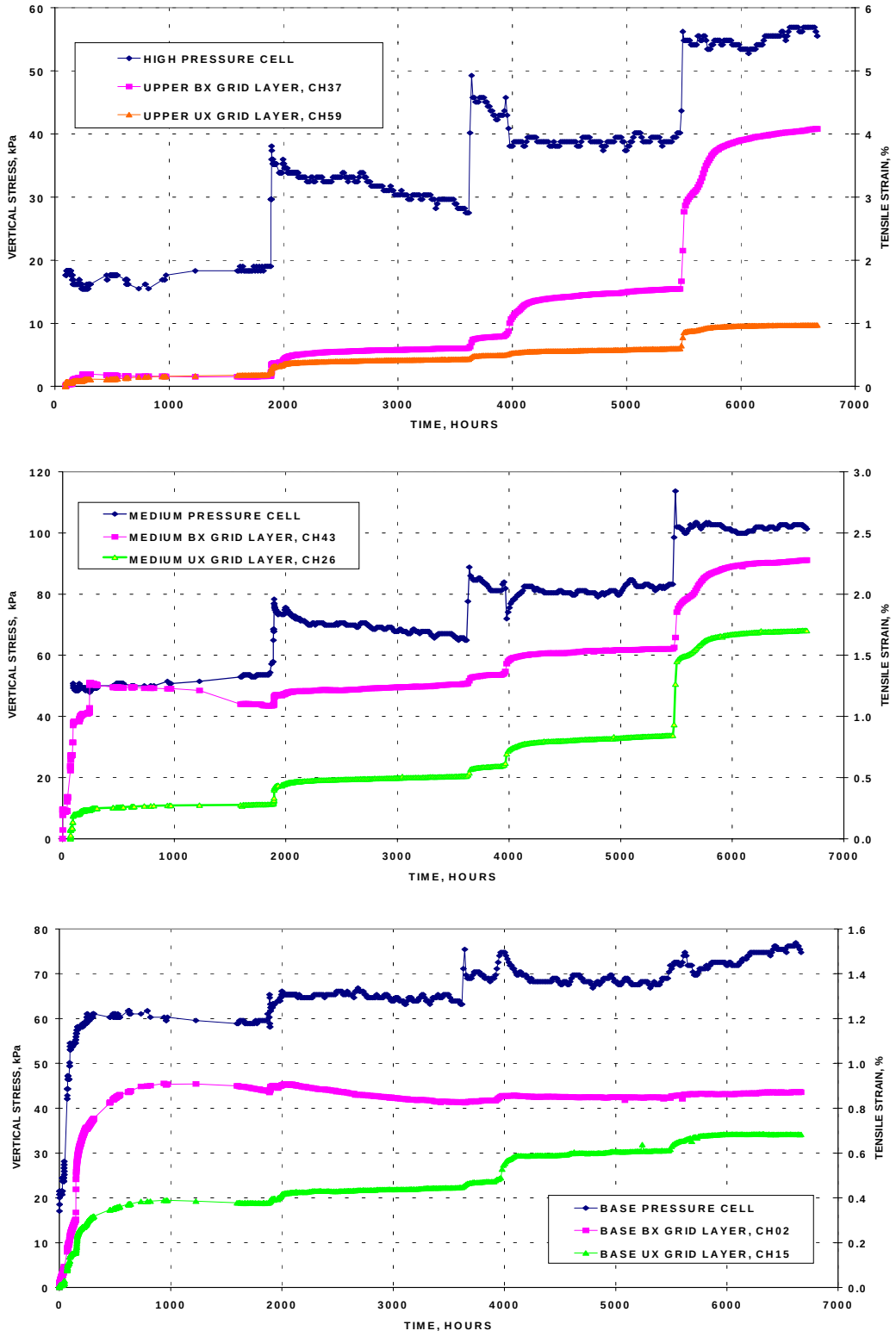

Figure 4. Comparison between total vertical pressure and strains at some instrumented locations of the GG45PE and the GG20PP geogrids.

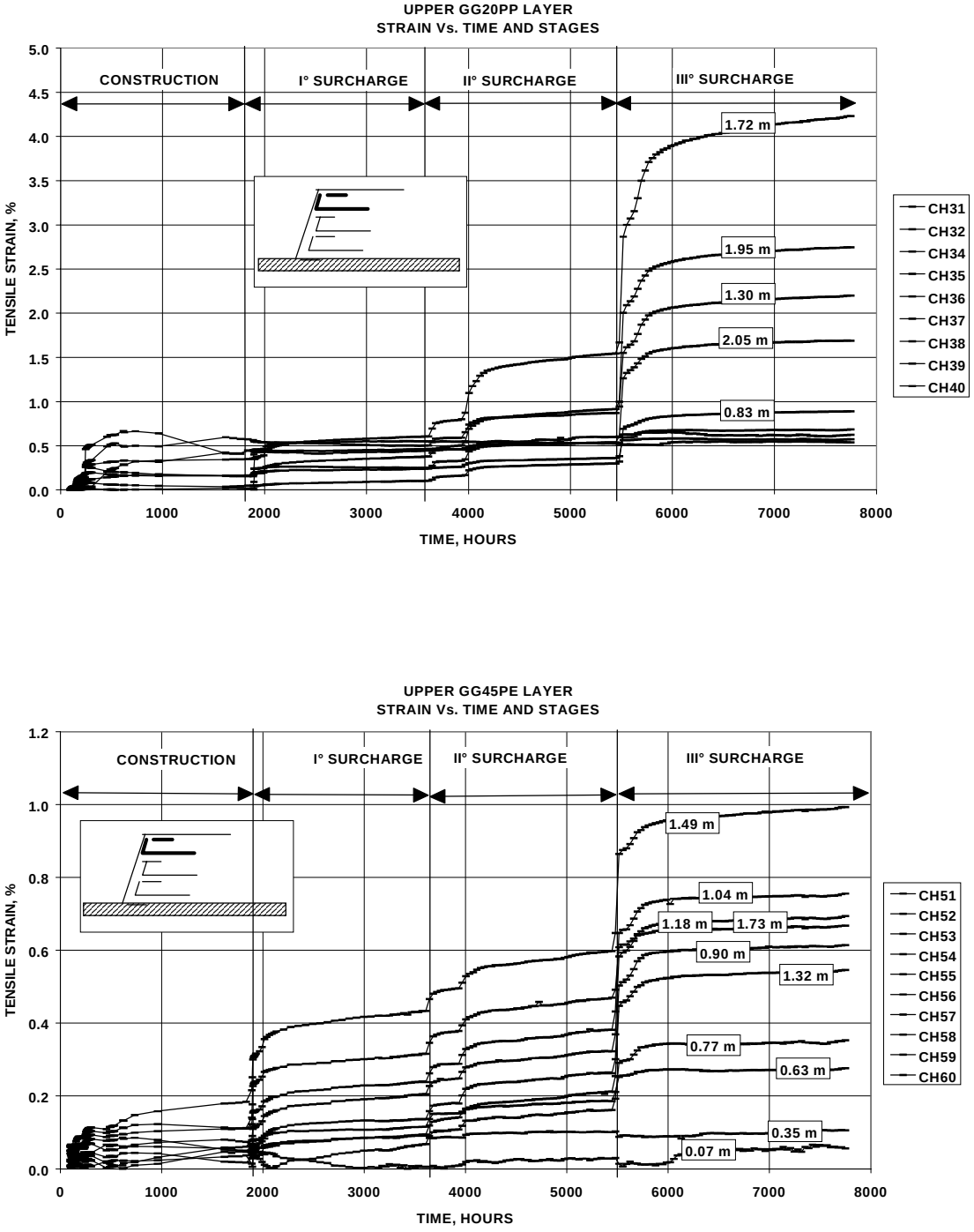

Figure 5. Tensile strains vs. time in the upper reinforcing layers for the GG45PE and the GG20PP geogrids. On the curves are shown the strain gages face distance

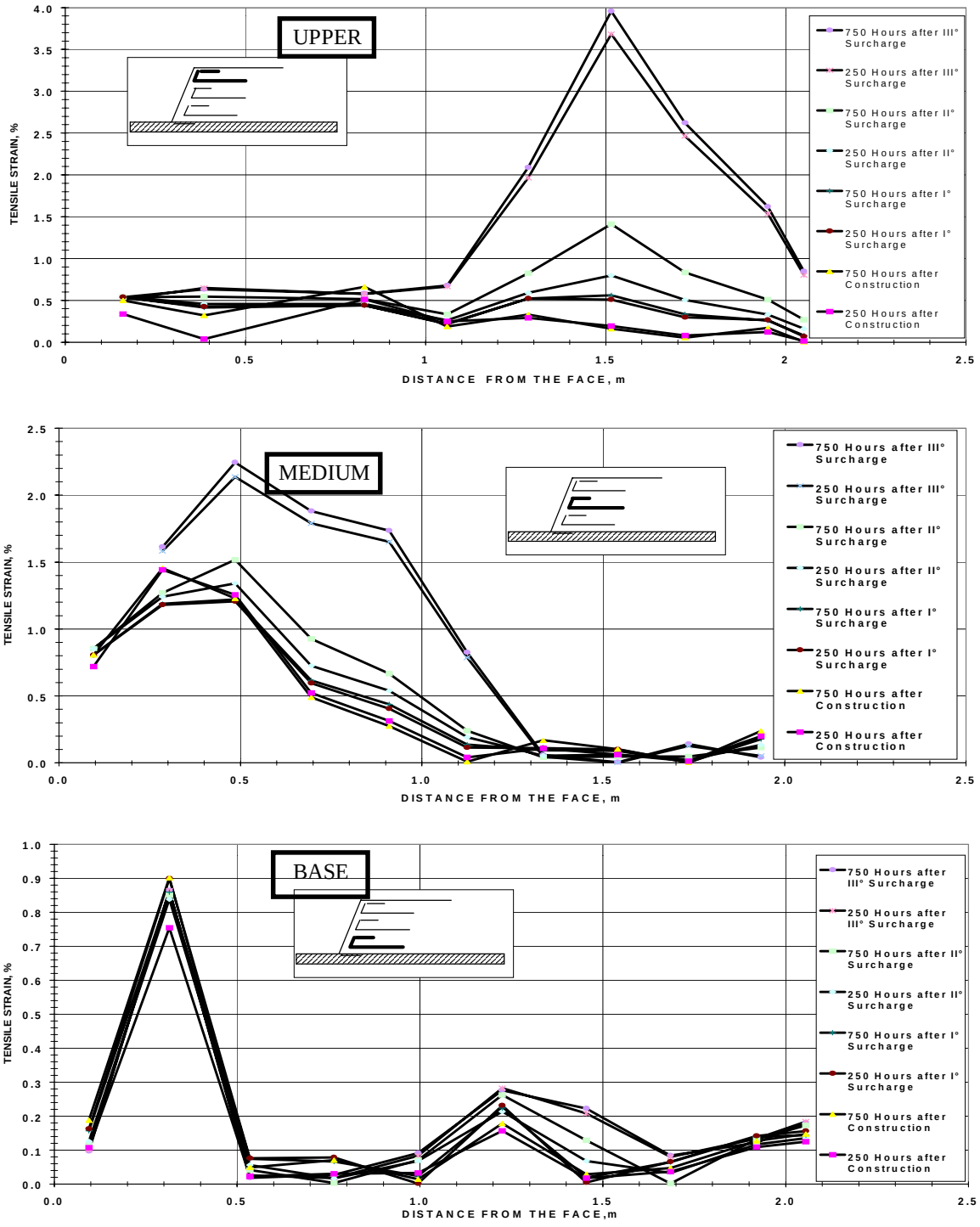

Figure. 6: Tensile strains vs. time along the GG20PP geogrid reinforcing layers.

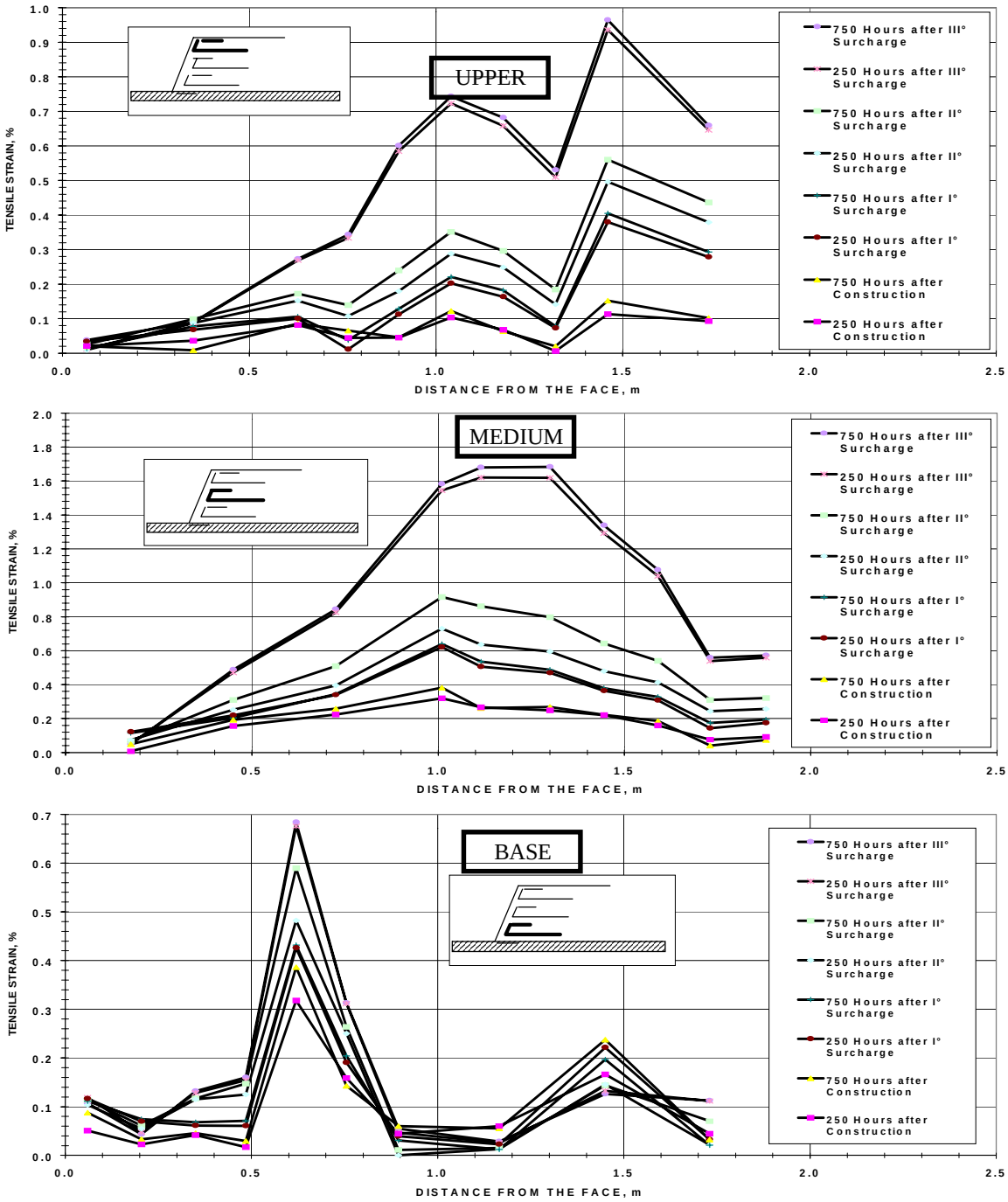

Figure 7. Tensile strains vs. time along the GG45PE geogrid reinforcing layers.

The maximum tensile strain achieved in each reinforcing layer indicates the location in which tension is greatest. Using this information, the location of the internal failure plan can be identified. The two slip surfaces obtained by this analysis are shown in Figures 8 and 9 as well as the failure surfaces considered in the design step, and the tensile strains measured. Moreover, the data in Figures 8 and 9 indicate that the reinforcing layers are stressed in a different way.

The actual mechanism of failure for GG45PE is pullout, as indicated by the multibase displacement data and by the low values of measured tensile strains (0.6-1.6% in Figure 7). The actual failure mechanism for GG20PP is tensile stress in the upper reinforcing layer as indicated by the high tensile strains measured (about 4.5 percent in Figure 6).

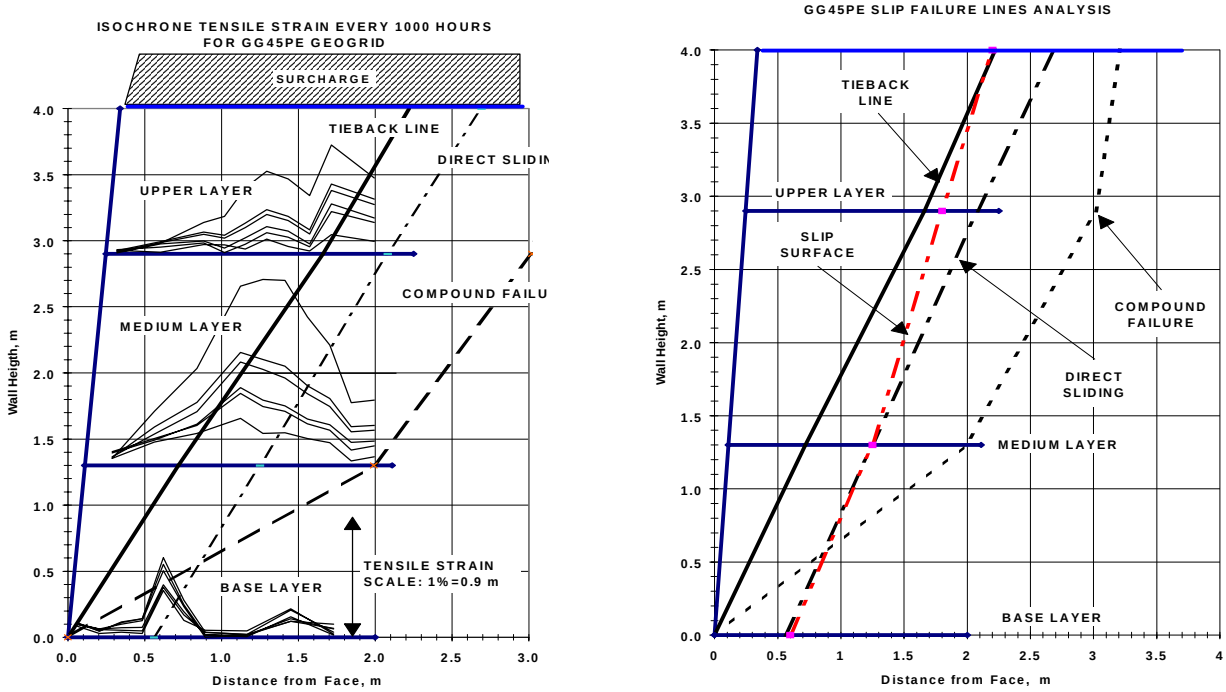

Figure 8. Localization of the actual slip surfaces inside the GG45PE reinforced wall.

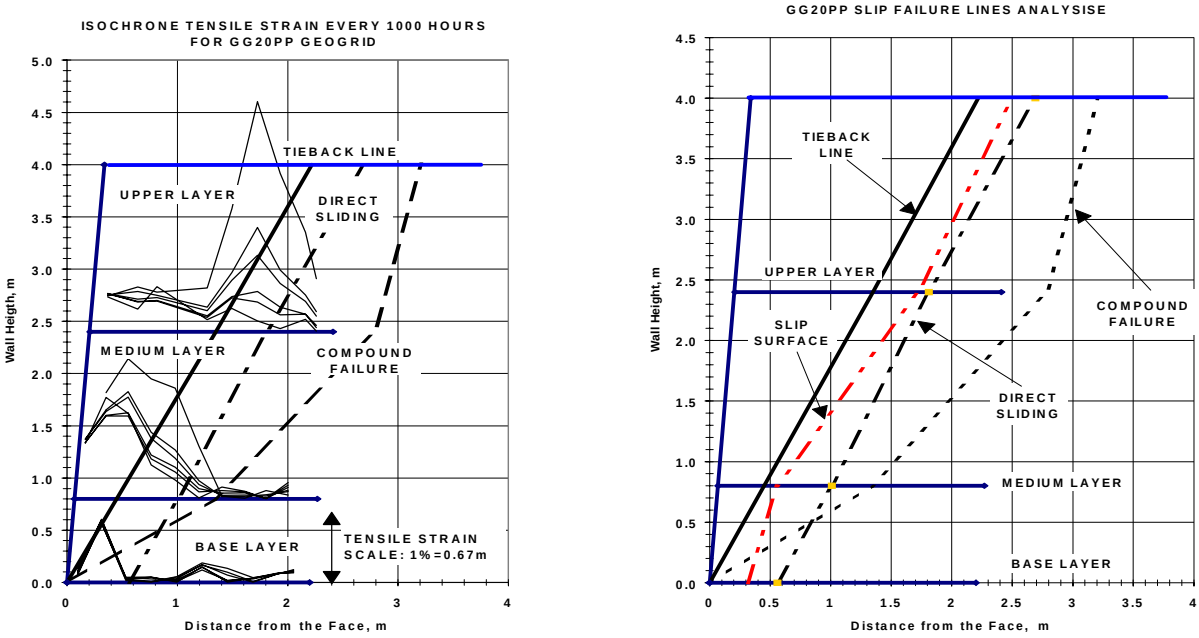

Figure 9. Localization of the actual slip surfaces inside the GG20PP reinforced wall.

FINITE ELEMENT ANALYSIS

For numeric modeling of the reinforced wall, a finite element analysis has been performed using the Abaqus software program. The wall cross section has been modeled using a mesh having 7000 nodes and 6300 elements. The analysis has been conducted using "plain strain" conditions and taking into consideration the history of loading of the reinforced structure and its surcharge (figure 10). The soil has been modeled using Drucker-Prager law and based upon the results of the pullout tests; a perfect interaction between soil and the geogrids has been considered (f_{po}=1.00).

In figure 11 are shown the horizontal stresses contour in a gray color scale. This figures show how the geogrid reinforcements greatly interact and reduce the horizontal tension in the reinforced wall. Figure 11 A shows the horizontal tension for the GG45PE on a deformed contour while figure 11 B shows the ones of GG20PP on the un-deformed cross-section.

In figure 12 are shown the behaviour of the horizontal strain within the reinforced mass. Following the maximum strain contour, it is possible to define the exact location and shape of the shear failure line. This line is passing through the maximum horizontal strains within the overall soil mass including the surcharge height. Thus the failure line is well defined, not only at the reinforcement location, but also within the overall structure.

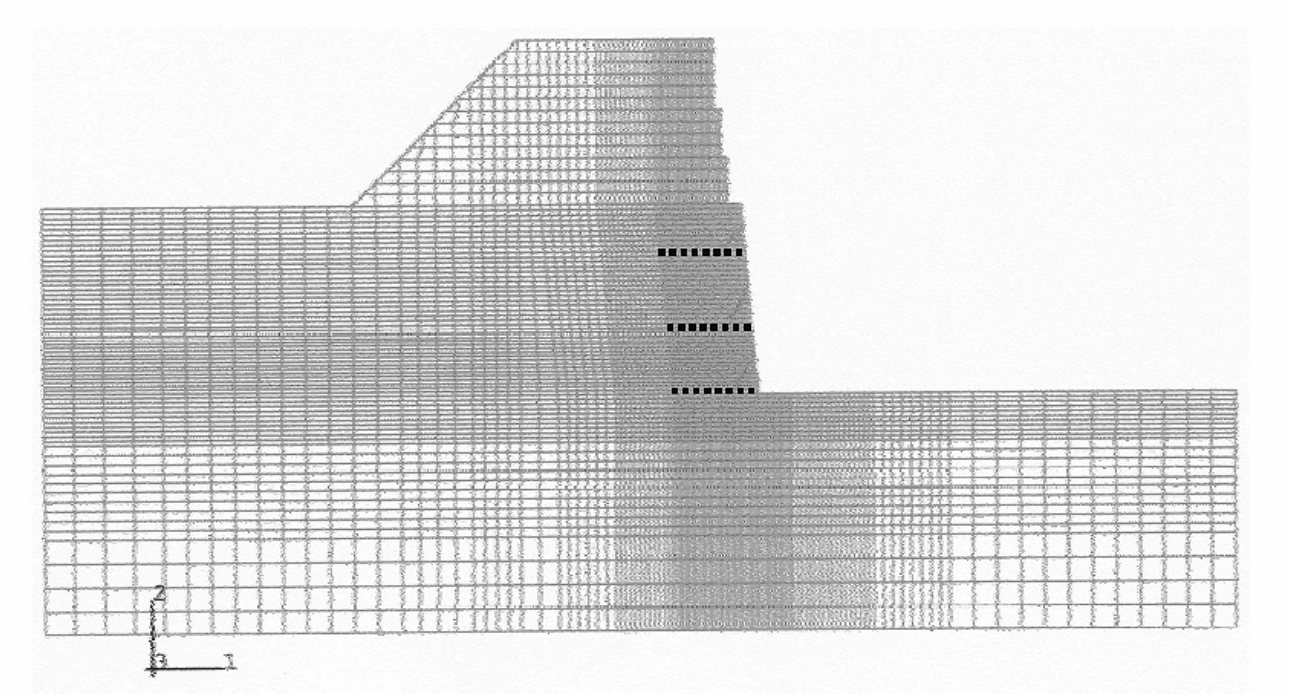

Figure 10: Mesh of the reinforced geogrid wall.

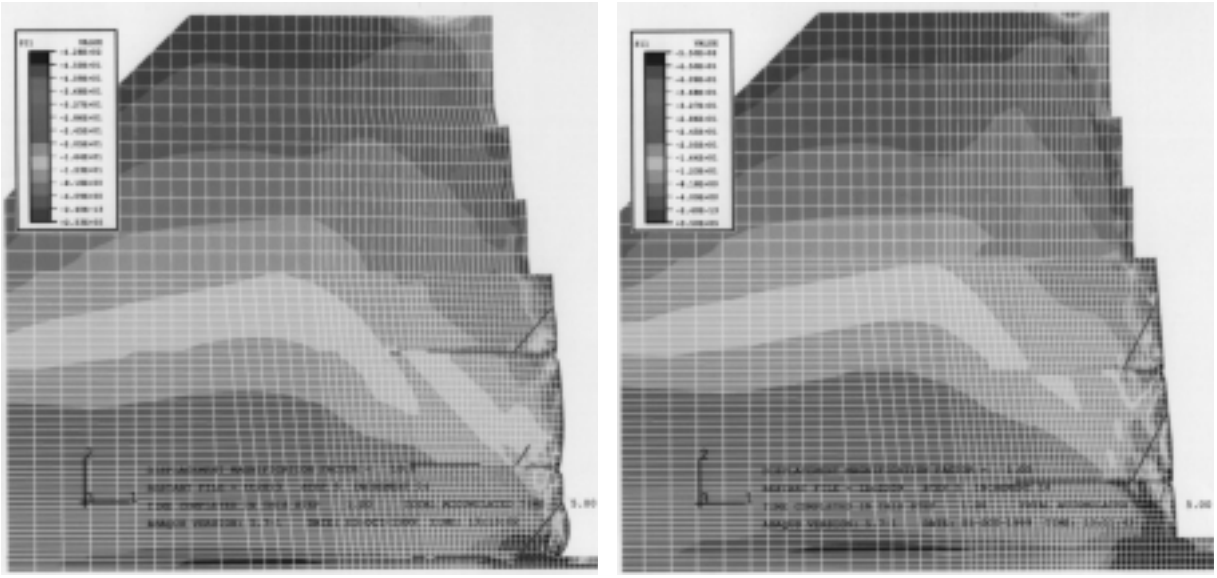

Figure 11: Horizontal Stresses for GG45PE (fig 11A) and GG20PP (fig 11B) geogrids

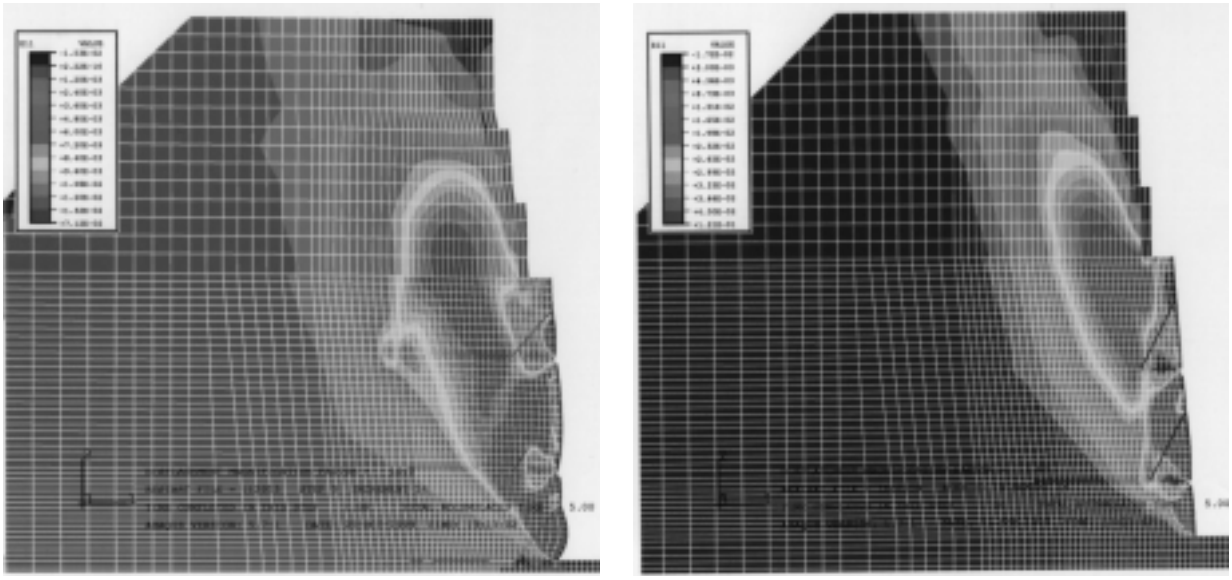

Figure 12: Horizontal Strains for GG45PE (fig 12A) and GG20PP (fig 12B) geogrids

In figure 13, it is shown the deformed mesh contour plot for both the reinforced cross section. The deformation has been amplified by a factor of 10 to highlight the shape of the deformation. A good correlation between the actual final shape of the structure and the output from the Abaqus program has been found.

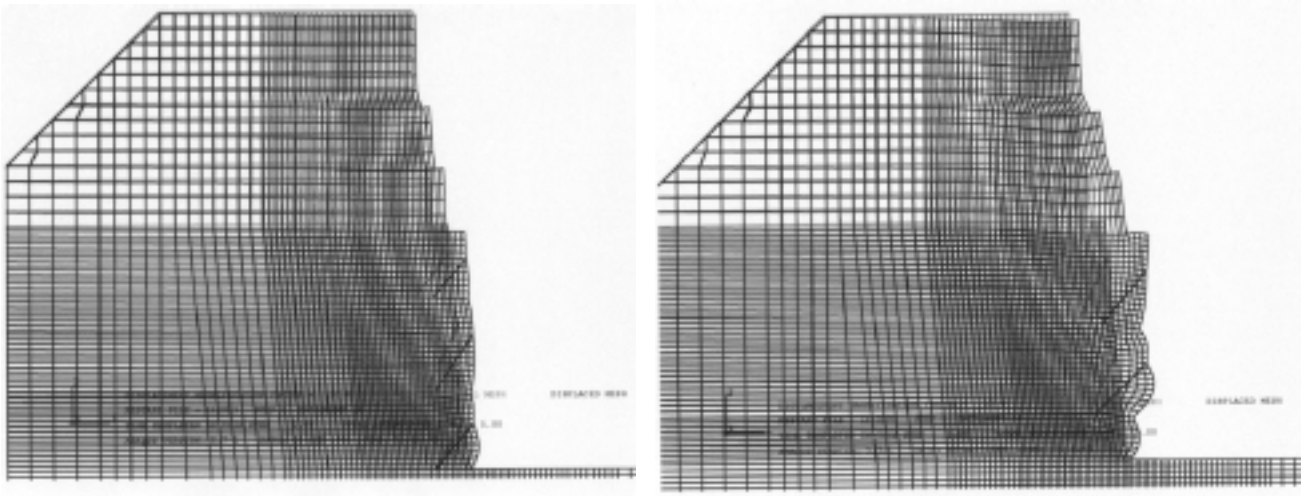

Figure 13: Deformed mesh contour plot for GG45PE (fig 13A) and GG20PP (fig 13B) geogrids

The Abaqus program has been used with great success to determine the vertical stress acting on the load cells. The Abaqus program, as shown in figure 14, provides a better interpretation of the experimental data. We must notice that the experimental data for the lower vertical pressure cell might have been reduced due to boundary effects of the nearby side of the wall. Figure 14 shows the vertical pressure acting on the upper load cell in comparison with the experimental data collected over a period of 16,000 hours and the one given by γh formula.

In figure 15 are given the comparisons, for both geogrids, of the FEM calculated horizontal strains (dotted lines) versus the actual experimental data (solid lines). The data are compared after 1,000 hours after the installation of the third surcharge step that is after about 7,000 hours after the beginning of the installation. This time has been selected to compare mainly the elastic portion of the geogrid visco-elastic strains, since the soil and the geogrids has been modeled with an elastic model. The level of accuracy in the prediction of the horizontal strains given by the Abaqus program is excellent. The program is able to estimate the level of horizontal strain with an error of about 15%. Anyhow the qualitative behavior is different since the Abaqus failure line is much steeper then the one measured empirically with the strain gages. This behavior is visible also in figure 12 and 16.

In figure 16, all the different failure lines are compared. The data presented have been obtained by the Abaqus analysis, the experimental data collected after 7,000 hours and by the Reslope program. The Reslope program has been run using the soil parameter resulting from the triaxial test (CD) on large diameter specimens, that are 45° soil friction angle (maximum input for Reslope) and cohesion of 5 kPa. The shape of the numerical solution failure line given by Abaqus is similar to the Tieback failure line given by the Reslope program, while the experimental lines lay within the Reslope Tieback and the Compound failure lines.

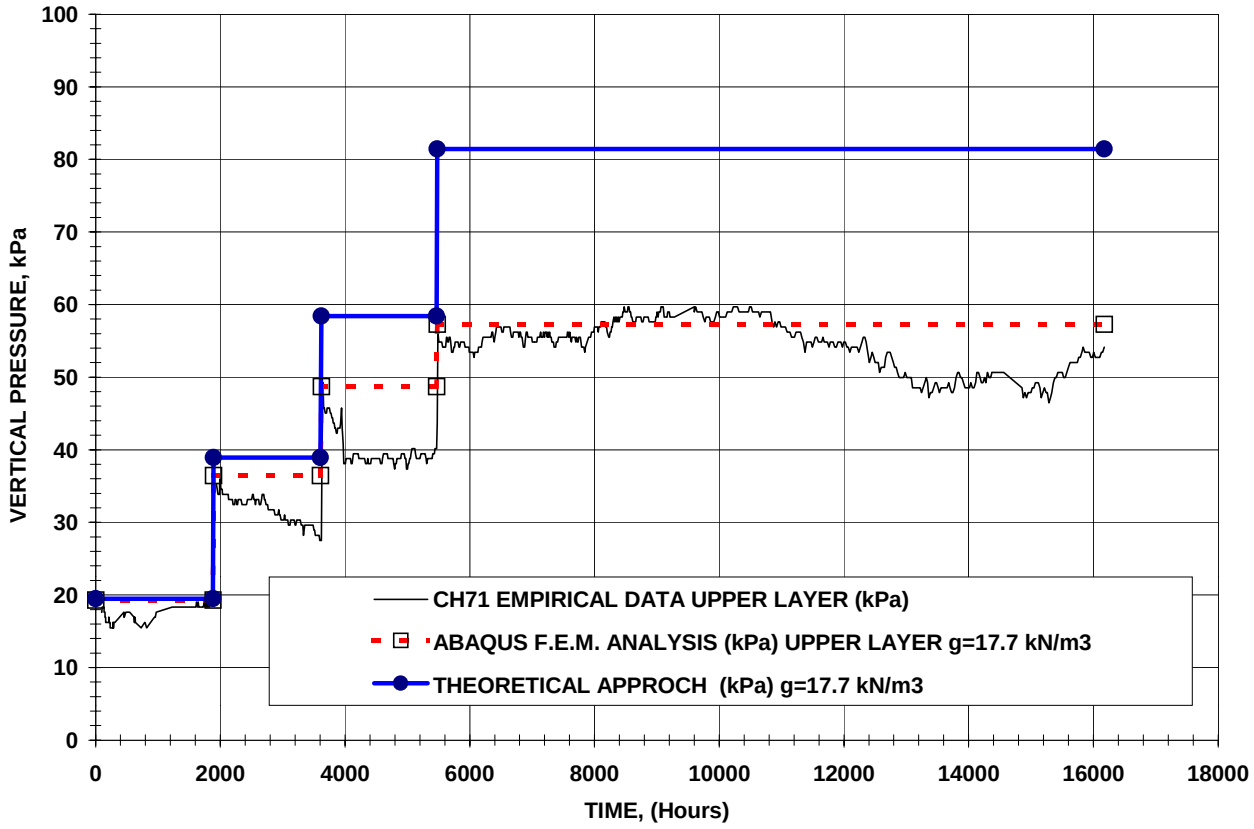

Figure 14: Vertical stress acting on the upper load cell.

CONCLUSIONS

Two sections of a vertical retaining wall, 4m high and 10m long, were constructed by reinforcing the backfill with two different types of geogrids. The reinforcing layers were instrumented with strain gauges, tensile geogrid load transducers and horizontal displacement sensors. Moreover, in order to measure the internal state of stress of the reinforced walls, total soil pressure transducers were installed inside the structure. Finally, the walls were brought to failure by surcharging them with 3.50m of compacted soil. The tensile strains collected inside the reinforced structures allowed the location of failure surfaces to be clearly identified. Two different failure mechanisms were identified: a pull-out mechanism failure for the GG45PE reinforced wall, and a tensile reinforcing failure for theGG20PP reinforced wall. Data have been collected up to a period of 16,000 hours. The behavior of the two structures has been analyzed by mean of a numerical program (Abaqus) and with the Reslope using soil parameters obtained by more accurate testing. This analysis shows that, using more accurate soil parameters, the wall was not yet at failure point. Anyhow the failure lines are similar among the programs being steeper for the Abaqus analysis and with the experimental data falling within the Reslope Tieback and Compound failure lines. The paper shows that the instrumentation and the long term observation of a large scale model may be considered a valuable tool in understanding the behavior of such a complex structures and that nowadays sophisticated FEM programs may provide good interpretation of data and valuable design even if they are not yet user friendly.

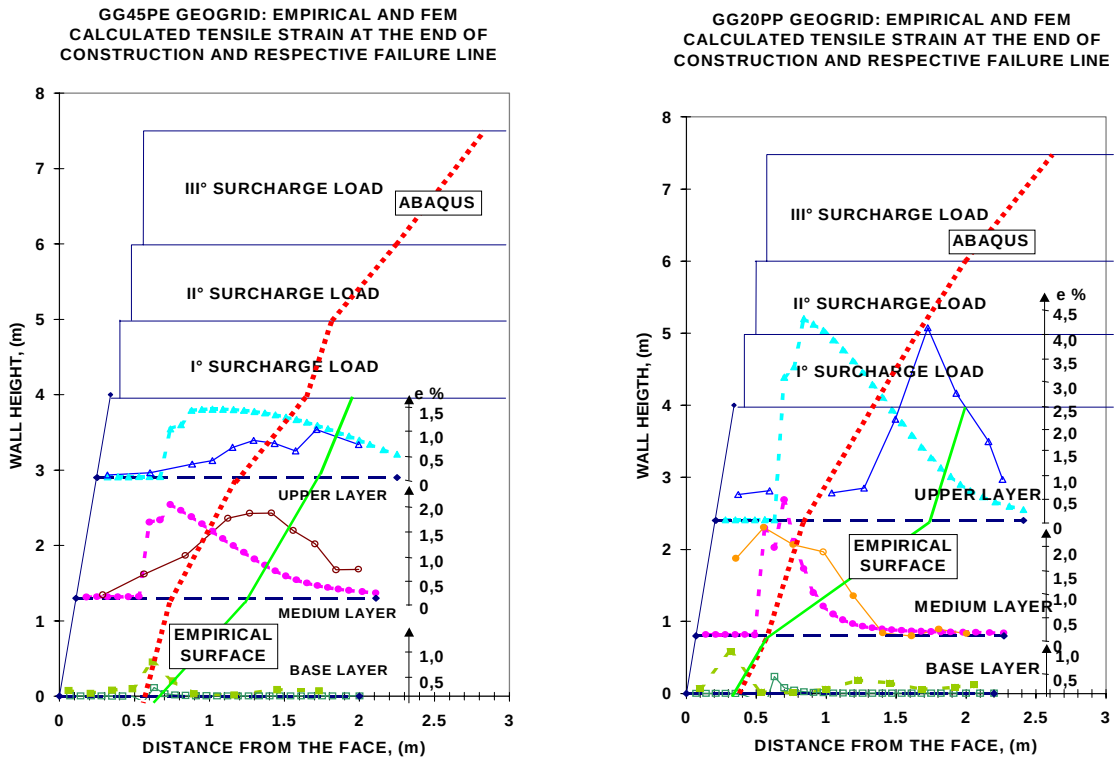

Figure 15: Comparison between measured and FEM calculated strains and failure lines

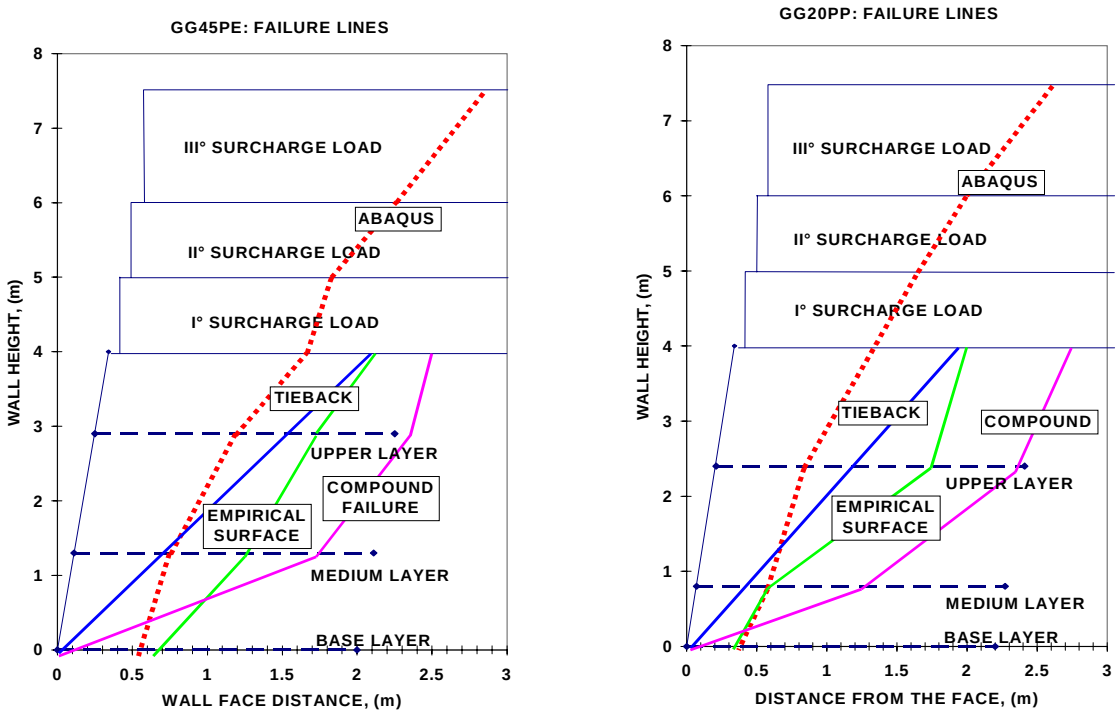

Figure 16: Comparison between measured, FEM and RESLOPE calculated failure lines

REFERENCES

ABAQUS/Standard (1997) User's Manual, Version 5.7, Hibbit, Karlsson & Sorensen, Inc., Pawtucket, USA.

Bonaparte, R., Holtz, R.D. and Giroud, J.P. (1987) " Soil Reinforcement Design Using Geotextiles and Geogrids", Geotextile Testing and the Design Engineer, ASTM STP 952, pp.69-116.

Carrubba, P., Moraci, N., Montanelli, F., (1999) "Instrumented Soil Reinforced Wall", Proceeding Geosynthetic '99, Boston, U.S.A., pp. 921-934.

Collin, J.G. (1986) " Earth Wall Design", Ph.D. Thesis, University of California, Berkley; U.S.A.

Jewell, R.A (1991) " Application of Revised Design Charts for Steep Reinforced Slopes ", Geotextiles and Geomembranes, Vol.10, n.4, pp.203-233.

Jewell, R.A., Paine, N., Woods, R.I. (1984) " Design Method for Steep Reinforced Embankments ", Polymer Grid Reinforcement in Civil Engineering, Thomas Telford, London, U.K., pp.70-81.

Leshchinsky, D., Perry, E.B. (1987) " A Design Procedure for Geotextile-Reinforced Walls ", Proceeding Geosynthetic '87, New Orleans, U.S.A., pp.95-107.

Leshchinsky, D. (1995) " RESLOPE " Design Manual, Department of Civil Engineering, University of Delaware, U.S.A.

Schmertmann, G.R., Chouery-Curtis, V.E., Johnson, R.D. and Bonaparte, R. (1987) " Design Charts for Geogrid-Reinforced Soil Slopes ", Proceeding Geosynthetic '87, New Orleans, U.S.A., pp.108-120.

Simac, M.R., Christopher, B.R., and Bonczkiewicz, C. (1990) " Instrumented Field Performance of a 6 m Geogrid soil wall " Proceeding 4th International on Geotextiles Geomembranes and Related Products, The Haughe, Holland, Vol.1, pp.53-59.